

# STATISTICAL MODEL FOR ESTIMATION OF INELASTIC RESPONSE SPECTRA

*By Zoran Milutinović\* and Hiroyuki Kameda\*\**

A simple method is developed for calculation of inelastic response spectra for arbitrarily predetermined values of ductility and damping. Period-dependent Ductility & Damping Reduction Factor (DDRF) is defined as a scaling factor that convert 5%-damping elastic response spectra into an inelastic response spectra for desired damping and ductility. It is formulated as a product of two functions interrelating the ductility, damping and natural period, and a period-band-dependent matrix of regression coefficients which are statistically quantified on the basis of Japanese strong motion data set. Influence of site effects on DDRF is studied by classifying the strong motion records according to the soil condition classification employed in the Japanese Earthquake Design Specifications for Highway Bridges. On this basis a closed-form statistical model is proposed for prediction of a site-dependent inelastic response spectra for a given soil condition, ductility and damping.

## 1. INTRODUCTION

Since the introduction of the concept of response spectrum into earthquake engineering (Beniof, 1934 and Biot, 1941), response spectra method has been widely used for the design of a vast majority of earthquake-resistant structures. It is a main tool for preliminary design, even when the final design is examined by time history response analysis method.

Structures exposed to earthquakes of moderate to severe intensity usually behave out of elastic range-inelastic. Inelastic deformations have a significant influence on structural stiffness and strength degradation, which in turn strongly affect mobilized energy absorption and energy dissipation capacities of the structure. However, elastic spectra based only on the peak response amplitudes computed for various damping factors do not incorporate any information on the amount of inelastic deformation structure can withstand before structural damage or failure occurs. They also do not implement informations on 'actual' - effective response level of structure exposed to earthquake action. Although not a response quantity, the ductility is recognized as a common measure of inelastic structural deformability that most directly affect design elastic requirements associated with the corresponding design forces.

This paper proposes a new parameter - ductility and damping reduction factor<sup>7)</sup> ( $C_{\mu h}$ ) - statistically quantified on the basis of the 5%-damping standard response ratio<sup>3),6)-7)</sup> computed from the Japanese strong motion data set<sup>1)</sup>. Subsequently, it is uncoupled into damping ( $C_h$ ) and ductility ( $C_\mu$ ) reduction factors<sup>6),7)</sup> and on that basis effects associated with damping and ductility are separately elucidated.

\* M. Eng., Assistant Professor, Institute of Earthquake Engineering and Engineering Seismology-IZIIS, Skopje, University "Kiril and Metodij", Skopje, Yugoslavia.

\*\* Member of JSCE Dr. Eng., Associate Professor, School of Civil Engineering, Kyoto University. (Yoshida-honmachi Kyoto)

Throughout this paper, bilinear systems with the rigidity of inelastic hardening region of 10 % elastic rigidity are used.

## 2. THEORETICAL BACKGROUND

Considering that a 5% critical damping is of particular essence for a majority of structural systems covered by seismic design codes, the ductility & damping reduction factor is formulated as a reduction factor which converts 5% damping elastic spectra into corresponding inelastic spectra for desired damping and ductility; i.e.,

$$\left. \begin{array}{l} S_A(\mu, h, T_0) = C(\mu, h, T_0) S_{AE}(h=5\%, T_0) \\ \text{or} \\ S_A = C_{\mu h} S_{AE} \end{array} \right\} \dots\dots\dots (1)$$

where:  $S_A = S_A(\mu, h, T_0)$  is an inelastic pseudo acceleration response spectrum,  $C_{\mu h} = C_{\mu h}(\mu, h, T_0)$  is the ductility and damping reduction factor (DDRF), and  $S_{AE} = S_{AE}(h=5\%, T_0)$  = damping elastic response spectrum,  $h$  = damping factor, and  $T_0$  = undamped natural period of linear vibration.

Let us denote a 5% damping zero-period normalized\* spectral shape (hereinafter referred to as a referent standard response ratio-RSRR) by  $\xi_r = \xi(h=5\%, T_0)$  and an inelastic zero-period-normalized spectral shape (hereinafter referred to as a standard response ratio-SRR) by  $\xi = \xi(\mu, h, T_0)$ , so that with  $A_p$  denoting the peak ground acceleration:

$$S_{AE} = \xi_r(h=5\%, T_0) A_p = \xi_r A_p \dots\dots\dots (2)$$

and

$$S_A = \xi(\mu, h, T_0) A_p = \xi A_p \dots\dots\dots (3)$$

Then  $\xi$ ,  $\xi_r$  and  $C_{\mu h}$  are interrelated as follows:

$$\left. \begin{array}{l} \xi(\mu, h, T_0) = C(\mu, h, T_0) \xi_r(h=5\%, T_0) \\ \text{or} \\ \xi = C_{\mu h} \xi_r \end{array} \right\} \dots\dots\dots (4)$$

Designating statistical estimates for  $\xi$  and  $C_{\mu h}$  by  $\hat{\xi}$  and  $\hat{C}_{\mu h}$ , respectively, the inelastic response spectra for desired ductility and damping can be estimated from:

$$S_A = U \hat{C}_{\mu h} \hat{\xi}_r A_p \dots\dots\dots (5)$$

where  $U$  is an uncertainty defined as:

$$U = U_c U_\xi \dots\dots\dots (6)$$

in which  $U_\xi$  is statistical uncertainty inherent in  $\xi_r$  and  $U_c$  is an error involved in modeling of  $C_{\mu h}$ .

## 3. STATISTICAL ANALYSIS

### (1) Modeling of RSRR ( $\xi_r$ )

On the basis of a bilinear load-deformation model with the hardening stiffness of 10 % of nominaelastic stiffness, the SRR curves were computed for ductilities:  $\mu=1, 1.5, 2, 3$  and 4; damping:  $h=5, 10, 15, 20$  and 40% of critical and 31 discrete period points from 0.1s to 5s<sup>7)</sup>. They were calculated as an arithmetic mean of a family of response ratio curves since it involves the least systematic bias of the scatter of individual data around the mean values. In such a way the SRR curves are defined as unbiased estimators which represent overall acceleration amplification of the strong motion data set employed for a given ductility and damping.

The SRR curve evaluated for  $\mu=1$  and 5% critical damping was selected as the RSRR curve. However, as a consequence of small damping, RSRR curve was found to fluctuate excessively with the period. Smoothing was performed by fitting a high order polynomial of the form:

\* Zero-period-normalized spectra are identical with the response spectra normalized by the peak input acceleration.

Table 1 List of Polynomial Coefficients  $a_k/E_q$  for the Japanese Strong Motion Data.

Coeff $\backslash$ n	S o i l C o n d i t i o n :																			
	Rock (JPN1-R)					Diluvial (JPN2-D)					Alluvial (JPN3-A)					Very Soft Deposite (JPN4-SD)				
	4	5	6	7	8	4	5	6	7	8	4	5	6	7	8	4	5	6	7	8
$a_0$	-0.6693	-0.6544	-0.6546	-0.6463	-0.6463	0.0457	0.0391	0.0387	0.0343	0.0345	0.1378	0.1702	0.1707	0.1928	0.1914	0.2722	0.3051	0.3051	0.3215	0.3219
$a_1$	-1.3452	-1.2945	-1.2554	-1.2559	-1.2599	-1.0234	-1.0460	-0.9865	-0.9865	-0.9730	-0.9489	-0.8389	-0.9190	-0.9188	-1.0102	-1.1069	-0.9948	-0.9989	-0.9987	-0.9728
$a_2$	1.1094	0.8158	0.8786	0.5050	0.5035	-0.8298	-0.6990	-0.6034	-0.4049	-0.4004	-1.3225	-1.9599	-2.0888	-3.0776	-3.1079	-2.1141	-2.7632	-2.7698	-3.5025	-3.4939
$a_3$	-0.1543	-0.6333	-0.9585	-1.2487	-1.1702	0.1685	0.3818	-0.1136	0.0406	-0.1961	-0.0353	-1.0754	-0.4075	-1.1756	0.4230	0.2817	-0.7773	-0.7434	-1.3126	-1.7653
$a_4$	-1.5097	-0.8750	-1.2671	0.7581	0.8069	0.1340	-0.1486	-0.7459	-1.8221	-1.9691	0.5280	1.9060	2.7111	8.0715	9.0650	1.2195	2.6225	2.6634	6.6360	6.3547
$a_5$		0.8129	1.3373	3.0693	2.7512		-0.3620	0.4368	-0.4835	0.4750		1.7651	0.6882	5.2728	-1.2018		1.7972	1.7425	5.1402	6.9736
$a_6$			0.5742	-2.0886	-2.3267			0.8749	2.2899	3.0071			-1.1794	-8.2277	-13.0722			-0.0599	-5.2835	-3.9118
$a_7$				-2.4522	-2.0929				1.3030	0.2203				-6.4908	0.8226				-4.8104	-6.8812
$a_8$					0.3063					-0.9229					6.2341					-1.7652
$\sigma$	0.0304	0.0261	0.0261	0.0252	0.0257	0.0240	0.0234	0.0225	0.0225	0.0230	0.0481	0.0329	0.0319	0.0229	0.0219	0.0508	0.0364	0.0371	0.0338	0.0344

$n$ =Order of Polynomials

$$\log \xi_r = \sum_{k=0}^n a_k (\log T_0)^k \dots \dots \dots (7)$$

It was found that polynomials of order higher than 4 give a satisfactorily small standard error over the entire period range. The higher the order of the polynomial is, the smaller certainly is the standard error over the range of short and intermediate periods of  $0.1 \text{ s} \leq T_0 \leq 0.8 \text{ s}$ . Trial and error analysis has shown that the 8<sup>th</sup> order polynomial give the best fit to the data. The polynomial coefficients  $a_k$  indispensable for generation of the  $\xi_r$  curves are summarized in Table 1. They are tabulated along with standard errors  $\sigma$  for order 4 through order 8.

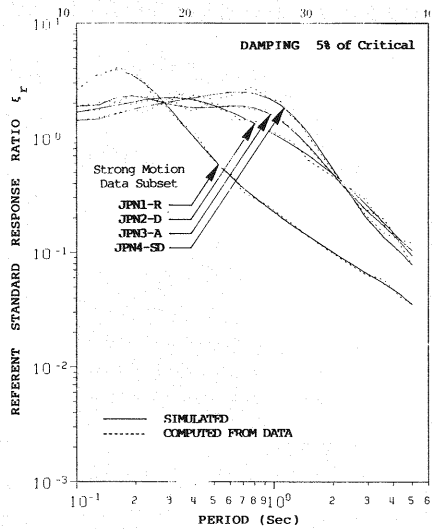


Fig.1 Referent Standard Acceleration Response Ratio  $\xi_r$  (RSRR) Curves.

Table 2 Tabular Presentation of Referent Standard Acceleration Response Ratio  $\xi_r$  (RSRR) Curves.

Period $T_0$ (sec)	S o i l C o n d i t i o n			
	Rock	Diluvial	Alluvial	Very Soft Deposite
	(JPN1-R)	(JPN2-D)	(JPN3-A)	(JPN4-SD)
0.10	2.603	1.671	1.892	1.418
0.13	3.647	1.801	1.932	1.459
0.16	3.906	1.921	2.236	1.619
0.19	3.565	2.039	2.318	1.761
0.22	3.013	2.136	2.247	1.868
0.25	2.471	2.201	2.130	1.951
0.28	2.015	2.234	2.021	2.019
0.31	1.654	2.237	1.939	2.080
0.34	1.374	2.216	1.884	2.137
0.37	1.158	2.178	1.853	2.191
0.40	0.990	2.126	1.839	2.244
0.44	0.820	2.045	1.841	2.310
0.48	0.695	1.956	1.854	2.371
0.52	0.600	1.866	1.873	2.422
0.56	0.527	1.777	1.890	2.463
0.60	0.469	1.691	1.901	2.491
0.64	0.422	1.610	1.905	2.506
0.68	0.384	1.533	1.899	2.507
0.72	0.353	1.462	1.883	2.494
0.76	0.326	1.396	1.857	2.468
0.80	0.303	1.334	1.822	2.429
0.94	0.244	1.149	1.646	2.216
1.08	0.205	1.004	1.426	1.929
1.22	0.177	0.886	1.207	1.626
1.36	0.156	0.788	1.011	1.342
1.50	0.139	0.705	0.846	1.096
2.20	0.090	0.423	0.396	0.415
2.90	0.067	0.268	0.240	0.207
3.60	0.054	0.181	0.169	0.135
4.30	0.044	0.131	0.126	0.102
5.00	0.035	0.104	0.094	0.078

Fig.1 compares the RSRR curves  $\xi_r$  estimated from Eq. (7) for  $n=8$  (solid lines) with those computed numerically from the Japanese strong motion data (dotted lines). Their numerical values for 31 discrete period points are tabulated in Table 2. Four data groups<sup>3),7)</sup> indicated in Fig.1 correspond to the site classification employed in the Japanese seismic design specifications for highway bridges<sup>2)</sup>. The abbreviations JPN1-R, JPN2-D, JPN3-A and JPN4-SD stand, respectively, for rock, diluvial, alluvial

and very soft deposit sites.

(2) Modeling of DDRF ( $C_{\mu h}$ )

Thin solid lines in Fig.2 show the DDRF curves  $C_{\mu h}$  computed for various damping factors and ductilities from

$$C_{\mu h} = \xi / \xi_r \dots\dots\dots (8)$$

for the JPN2-D data set. As a consequence of smoothing performed on RSRR by Eq. (7), it appears that  $C(\mu=1, h=5\%, T_0)$  strongly fluctuate around unity.  $T_0$  maintain the condition that  $C_{\mu h}=1$  for 5% damping and  $\mu=1$ , it was assumed that  $C(\mu=1, h=5\%, T_0)$  is equal to unity over the entire period range (Figs.2 and 7). Dotted lines in Fig.2 represent the  $C_{\mu h}$  curves obtained through normalizing  $\xi$  values relative to  $\xi(\mu=1, h=5\%, T_0)$  computed directly from the data. In order to determine a general ; tendency of  $C_{\mu h}$  curves, a new set of high order polynomials of form

$$C_{\mu h} = \sum_{k=0}^n d_k (\log T_0)^k \dots\dots\dots (9)$$

was drawn through the data evaluated by Eq. (8). For  $n=8$ , modeled  $C_{\mu h}$  curves are indicated by heavy solid lines in Fig.2. These  $C_{\mu h}$  were used as a data base for deriving  $C_{\mu h}$  statistical model for their estimation.

Assuming a linear relation between the logarithms of  $C_{\mu h}$  and  $\mu$  as well as considering that for any discrete period point,  $C(\mu=1, h=5\%, T_0)$  should be equal to unity, the DDRF values obtained from Eq. (9) for  $n=8$  were regressed by using :

$$\log C_{\mu h} = a(h, T_0) + b(h, T_0) \log \mu \dots\dots\dots (10)$$

Regressions were performed for all 31 discrete period points in the range of  $0.1 \leq T_0 \leq 5$  s separately for five damping factors.

Typical  $C_{\mu h}$  data and fitted regression lines for JPN2-D data set are presented in Fig.3 for a selected period of 0.8 s.

Ductility - independent regression coefficients  $a(h, T_0)$  and  $b(h, T_0)$  depend strongly on period and damping (Figs.4 and 5). The period-dependence (Fig.4) is generally irregular and can hardly be modeled by a single linear regression line. In contrast, a high linear dependence can be observed in regard to damping (Fig.5) for all discrete period points considered.

In order to separate the effects of the period and the damping, regression analysis was performed for 31 discrete period points

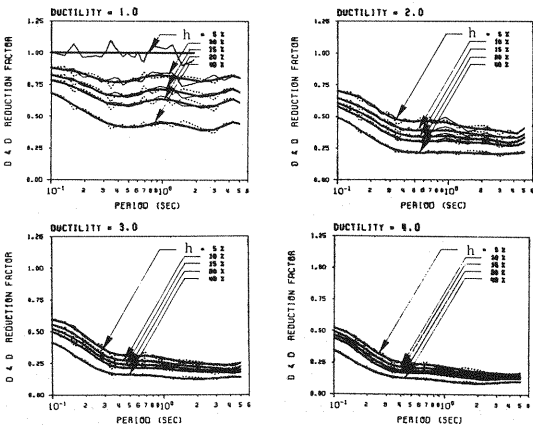


Fig.2 Ductility & Damping Reduction Factor  $C(\mu, h, T_0)$ /DDRf/Curves.

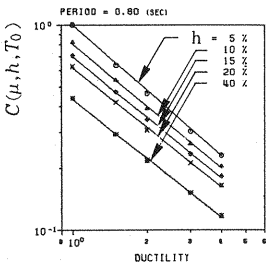


Fig.3 Dependence of  $C(\mu, h, T_0)$  on  $\mu$  for JPN2-D Strong Motion Data Set  $/T_0=0.8$  s/.

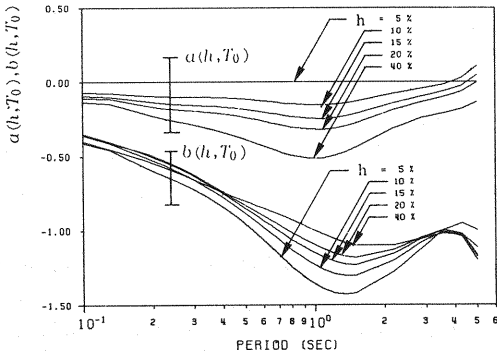


Fig.4 Dependence of  $a(h, T_0)$  and  $b(h, T_0)$  on  $T_0$  for JPN2-D Strong Motion Data Set.

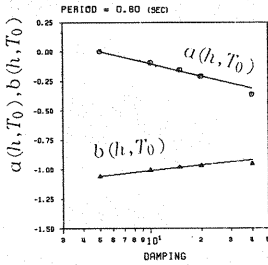


Fig.5 Dependence of  $a(h, T_0)$  and  $b(h, T_0)$  on  $h$  for JPN2-D Strong Motion Data Set/ $T_0=0.8s$ .

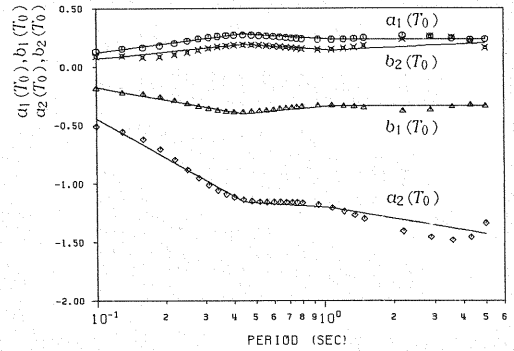


Fig.6 Dependence of  $a_1(T_0)$ ,  $b_1(T_0)$ ,  $a_2(T_0)$  and  $b_2(T_0)$  on  $T_0$  for JPN2-D Strong Motion Data Set.

by using the expression

$$\begin{bmatrix} a(h, T_0) \\ b(h, T_0) \end{bmatrix} = \begin{bmatrix} a_1(T_0) & b_1(T_0) \\ a_2(T_0) & b_2(T_0) \end{bmatrix} \begin{bmatrix} 1 \\ \log h \end{bmatrix} \quad (11)$$

From the results, it was found that the data scatter around  $a(h, T_0)$  and  $b(h, T_0)$  increases with increasing damping. For this reason, two separate models were proposed<sup>7</sup>; one to deal with low damping region, and the other with high damping. The damping level of about 25 % of critical is suggested for a border between the two models. In the following, only the results derived from the low-damping statistical model are presented. Ductility-damping independent regression coefficients  $a_1(T_0)$ ,  $b_1(T_0)$ ,  $a_2(T_0)$  and  $b_2(T_0)$  are also period-dependent (Fig.6). In order to decrease dispersion inherent in modeling of aforelisted coefficients, a set of segmental-piecewise-linear regression lines were used for their modeling. Over a single segment, regression lines represented by :

$$\begin{bmatrix} a_1(T_0) \\ b_1(T_0) \\ a_2(T_0) \\ b_2(T_0) \end{bmatrix} = \begin{bmatrix} a_{11} & a_{12} \\ b_{11} & b_{12} \\ a_{21} & a_{22} \\ b_{21} & b_{22} \end{bmatrix} \begin{bmatrix} 1 \\ \log T_0 \end{bmatrix} \quad (12)$$

were fitted to data. It was found that a three-segmental piecewise linear regression model gives a satisfactory fit to the data and is simple enough for practical application. Continuity of regression lines were maintained at boundary points of adjacent segments. The values of the regression coefficients in Eq. (12) are summarized in Table 3 in accordance with determined period ranges<sup>7</sup> depending on the soil condition type.

Table 3 Summary of Regression Coefficients  $a_{11}$ ,  $a_{12}$ ,  $b_{11}$ ,  $b_{12}$ ,  $a_{21}$ ,  $a_{22}$ ,  $b_{21}$  and  $b_{22}$  /Eqs. 12, 13, 16 and 17/for the Japanese Strong Motion Data Sets.

Soil Condition	Period Range (sec)	$a_{11}$	$a_{12}$	$a_{21}$	$a_{22}$	$b_{11}$	$b_{12}$	$b_{21}$	$b_{22}$
Rock (JPN1-R)	0.10-0.19	0.7298	0.4630	-1.0442	-0.6624	-4.1141	-3.1581	1.1975	0.9299
	0.19-0.44	0.0621	-0.4628	-0.0887	0.6623	-0.6320	1.6699	-0.0831	-0.8455
	0.44-5.00	0.2438	0.0469	-0.3488	-0.0671	-1.2569	-0.0827	0.2174	-0.0027
Diluvial (JPN2-D)	0.10-0.44	0.3694	0.2452	-0.5285	-0.3508	-1.5479	-1.1048	0.2588	0.1900
	0.44-1.08	0.2397	-0.1186	-0.3429	0.1697	-1.2019	-0.1345	0.1458	-0.1271
	1.08-5.00	0.2357	0.0005	-0.3372	-0.0008	-1.1954	-0.3295	0.1384	0.0935
Alluvial (JPN3-A)	0.10-0.44	0.2946	0.0778	-0.4215	-0.1114	-1.1994	-0.4405	0.2741	0.0329
	0.44-1.08	0.3055	0.1085	-0.4371	-0.1551	-1.4806	-1.2294	0.2889	0.0744
	1.08-5.00	0.3125	-0.0997	-0.4470	0.1427	-1.5283	0.1975	0.2903	0.0297
Very Soft Deposit (JPN4-SD)	0.10-0.44	0.3373	0.2126	-0.4826	-0.3043	-1.3061	-0.8468	0.2358	0.1327
	0.44-1.08	0.3738	0.3149	-0.5347	-0.4504	-1.6745	-1.8801	0.4560	0.7503
	1.08-5.00	0.4026	-0.6492	-0.5760	0.7857	-1.7874	1.4977	0.5166	-1.0622

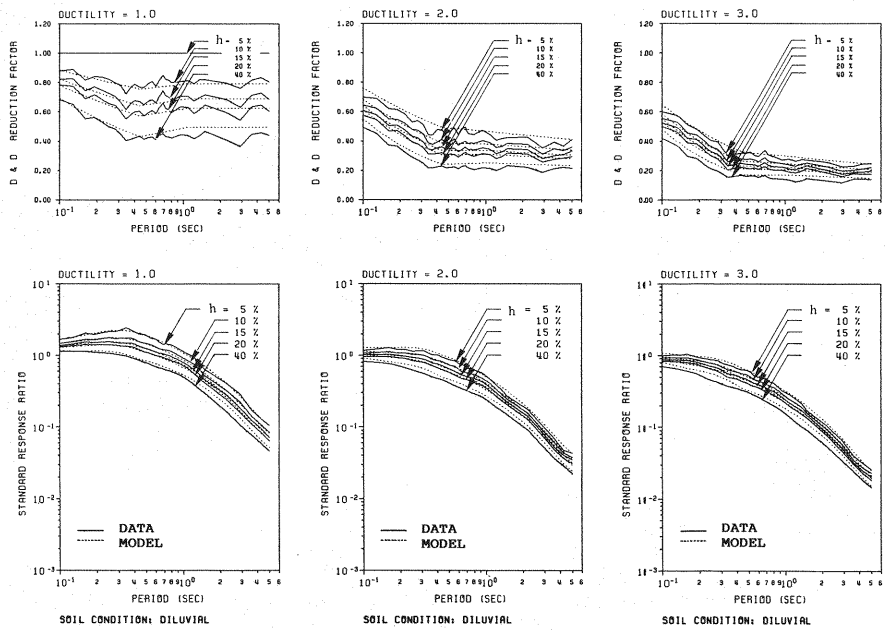


Fig. 7 Ductility & Damping Reduction Factor /DDRF/ and Standard Acceleration Response Ratio /SRR/ Curves.

Combining Eqs. (10), (11) and (12) the following expression for estimation of DDRF was obtained :

$$\log C_{\mu h} = [1 \quad \log \mu] \begin{bmatrix} a_{11} & a_{12} & b_{11} & b_{12} \\ a_{21} & a_{22} & b_{21} & b_{22} \end{bmatrix} \begin{bmatrix} 1 \\ \log T_0 \\ \log h \\ \log h \log T_0 \end{bmatrix} \dots\dots\dots (13)$$

Introducing Eqs. (13) and (7) into Eqs. ( 4 ) we propose the following expression for estimating of  $\xi(\mu, h, T_0)$  for desired ductility and damping factors :

$$\xi(\mu, h, T_0) = C_{\mu h} \xi_r = 10^{(\log C_{\mu h} + \sum_{k=0}^8 a_k (\log T_0)^k)} \dots\dots\dots (14)$$

The differences between the estimated  $C_{\mu h}$  and  $\xi$  curves and those computed numerically from the data (Fig.7) are not significant for low and intermediate range of damping factors. Modeling error computed in terms of standard error was found to be within 0.015~0.12, irrespective of data set considered and ductility or damping employed in the analysis. The significant discrepancy appears only in a high damping range, say  $h=30 \sim 40$  % critical damping. This is expectable since the results presented herein have been obtained from the low-damping statistical model. If the  $C_{\mu h}$  curves for high damping are to be estimated, the high-damping statistical model<sup>7)</sup> should be applied. However, from the view point of the practical application, it must be pointed out that using the model presented in this paper is on the conservative side when extended to high damping ranges (say 40 %) since the modeled SRR values in this damping range are larger than the data.

4. DISCUSSIOIN AND RESULTS

In the above we have qualitatively and quantitatively described ductility & damping reduction factor. As previous works<sup>4),5),-6),8),10)</sup> are not organized with such a comprehensive treatment of the joint effects associated with damping and ductility, comparison of results obtained in this study was enabled through uncoupling  $C_{\mu h}$  in the following form :

$$C_{\mu h} = C_h C_{\mu} = C_h(T_0) C_{\mu}(h, T_0) = 10^{\alpha(h,T_0)} \mu^{b(h,T_0)} \dots\dots\dots (15)$$

where :  $C_h = C_h(T_0)$  is the damping reduction factor converting a 5%-damping elastic spectrum into an

elastic spectrum for desired damping, and  $C_\mu = C_\mu(h, T_0)$  is the ductility reduction factor which converts an elastic spectrum into as corresponding inelastic spectrum for desired ductility. Note that  $C_\mu$  is still under an effect of damping as a cross-effect term of damping and ductility on  $C_{\mu h}$ . However, it will be seen, Fig.8, that the effect of  $h$  on  $C_\mu$  is minor. Thus,  $C_h$  and  $C_\mu$  may be represented by :

$$\log C_h = [1 \quad \log h] \begin{bmatrix} a_{11} & a_{12} \\ b_{11} & b_{12} \end{bmatrix} \begin{bmatrix} 1 \\ \log T_0 \end{bmatrix} \dots \dots \dots (16)$$

$$\log C_\mu = [1 \quad \log h] \begin{bmatrix} a_{21} & a_{22} \\ b_{21} & b_{22} \end{bmatrix} \begin{bmatrix} 1 \\ \log T_0 \end{bmatrix} \log \mu \dots \dots \dots (17)$$

The transient region of the  $C_\mu$  and  $C_h$  curves displayed in Fig. 8 correspond approximatively to the overall predominant period range of the strong motion records considered in JPN2-D data set. Comparing the results obtained for other data sets<sup>7)</sup> one can observe a migration of transient regions toward long period regions with decrease in ground stiffness. This is reasonable because the predominant period range of surface ground motions is dominantly controlled by stiffness properties of the deposits where they were recorded. Irrespective of the data set considered, general behavior of  $C_h$  and  $C_\mu$  curves is similar; decrease in  $C_h$  and  $C_\mu$  values with the period as far as the predominant period range and thereafter slight increase or at least less rate of decrease with the period. This tendency can be explained from the view point of the resonance curve<sup>7)</sup>.

Fig.8 also compares a spectral behavior of  $C_h$  factor with the damping reduction factors proposed by Kawashima et. al.<sup>4),5)</sup> They have developed a period-dependent reduction factor, and a period-independent reduction factor, denoted herein, respectively, by  $C_{h k1}(T_0, h)$  and  $C_{h k2}(h)$  :

$$C_{h k1}(T_0, h) = \left( \frac{1.5}{40h+1} + 0.5 \right) \beta(T_0, h)^{\left( \frac{1}{300h+8} - 0.8h \right)} \dots \dots \dots (18)$$

and

$$C_{h k2}(h) = 0.983(h/0.05)^{-0.270} \dots \dots \dots (19)$$

Apparent discrepancy between the results of this study ( $C_h$ ) and those by Kawashima et. al. ( $C_{h k1}$  and  $C_{h k2}$ ) may be observed over the entire period range in Fig.8. Disagreement in long period range, say  $T_0 \geq 1.5$  s is natural because the Kawashima et. al. 's results are based on absolute acceleration spectra, whereas those from this study are based on pseudo acceleration spectra. However, the disagreement in the range of shorter periods will need some discussion. The authors have an opinion at this time that the results of this study has a more appropriate physical basis, since the zero-period damping reduction factor should converge to unity.

The ductility reduction factor  $C_\mu$  computed from Eq. (17) has been averaged over certain period

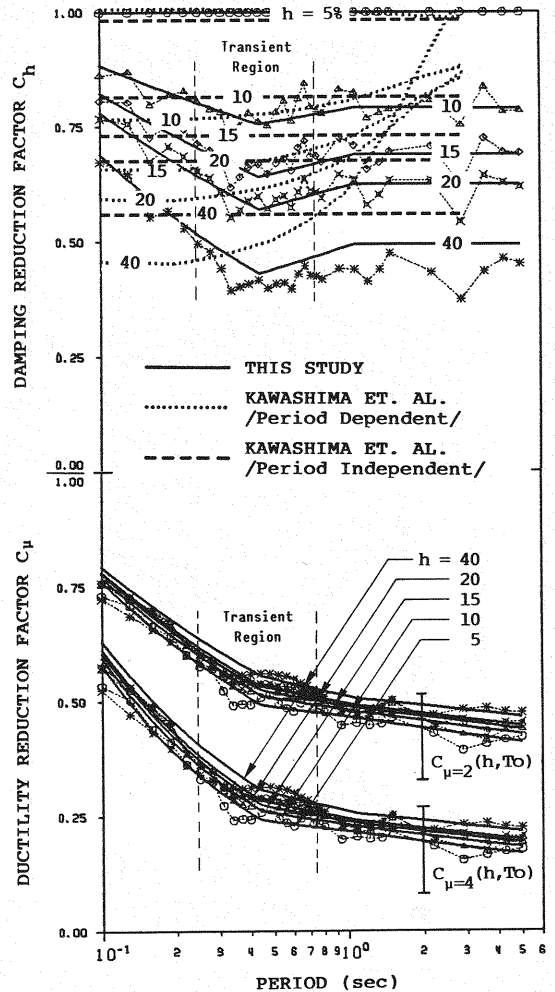


Fig.8 Spectral Behavior of  $C_h$  and  $C_\mu$  Reduction Factors.

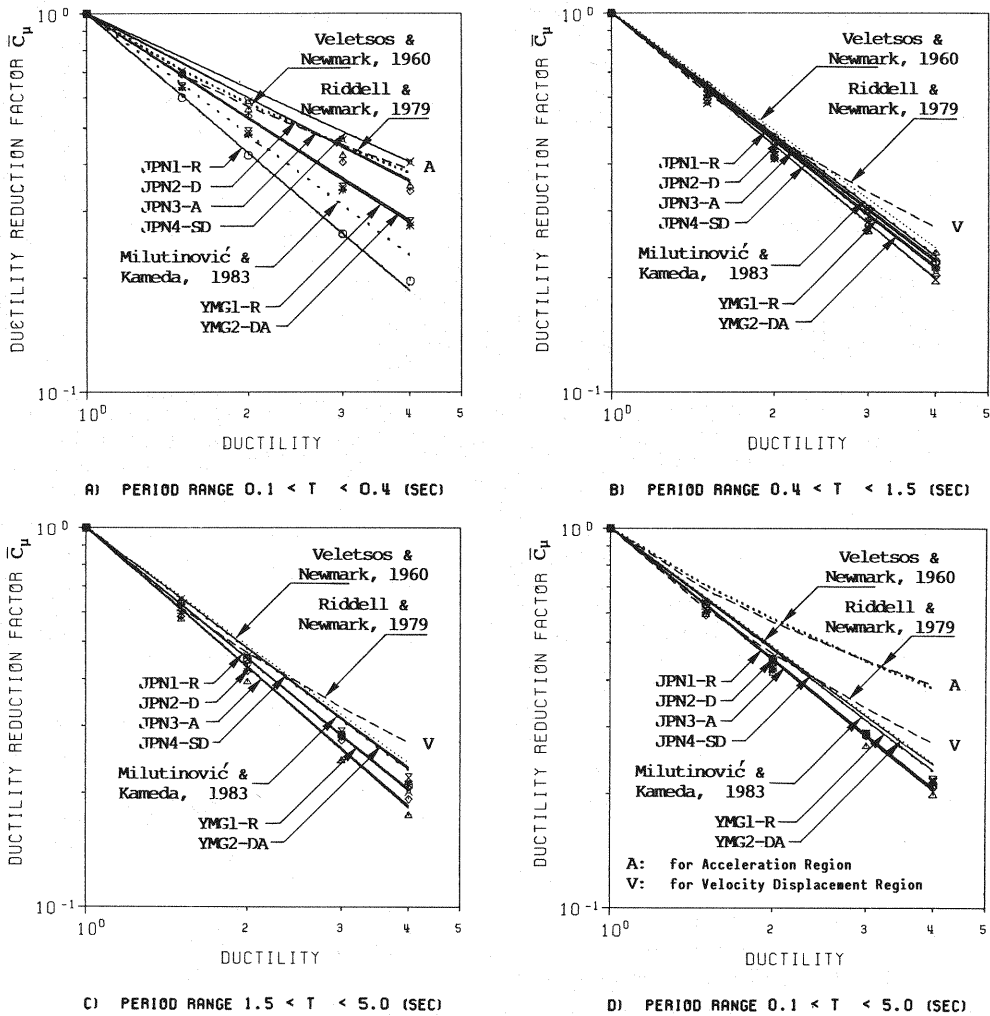


Fig. 9 Site-Dependent Average Ductility Reduction Factors ( $\bar{C}_\mu$ ) for the Japanese (JPN) and the Montenegro, Yugoslavia (YMG) Strong Motion Data Sets (5% Critical Damping). Symbols designate  $\bar{C}_\mu$  values computed from the data for various soil conditions. Corresponding modeled  $\bar{C}_\mu$  points are connected by solid lines.

ranges and the average values  $\bar{C}_\mu$  are displayed in Fig. 9 (marked by JPN1~JPN4). The period ranges determined in accordance with the soil condition classification in this study<sup>7)</sup> are: 0.1s~0.4s, 0.4s~1.5s and 1.5s~5.0s which approximately correspond, respectively, to acceleration, velocity and displacement spectral regions<sup>8,10)</sup>. Fig. 9 also shows the average for the entire period range of 0.1s~5.0s.

From these results it is apparent that the effect of soil condition is remarkable in the short period range 0.1s~0.4s, whereas with increasing period site-dependence of  $C_\mu$  factor lessens.

Besides the Japanese data, the Montenegro, Yugoslavia strong motion data<sup>9)</sup> were analyzed in the same manner. Results are parallelly presented in Ref. 7. as well as they are shown in Fig. 9 (marked YMG1 and YMG2). The results for the Montenegro data behave somehow in-between the JPN1 and JPN2 data for short period range of 0.1s~0.4s. For longer periods they are quite similar with overall results obtained from the Japanese strong motion data.

Fig. 9 compares results of this study with some results of former studies on the ductility reduction factor. It can be concluded that Veletsos & Newmark<sup>10)</sup> and, later improved Riddell & Newmark<sup>8)</sup> rules, proposed for



construction of inelastic design response spectra, generally agree well for periods longer than 0.4s. However, it should be pointed out that their results for acceleration spectral range (0.1s~0.4s) agree with only a part of the results of this study which depend largely on the soil condition.

Finally, the 5%-damping Milutinović & Kameda<sup>6)</sup> model, based on the Montenegro data, is compared. Observe that it is satisfactorily consistent with the data, irrespective of period range or data set considered.

## 5. CONCLUSIONS

The conclusions of this study may be summarized as follows, under the assumption of bilinear systems with the inelastic to elastic rigidity ratio of 10%.

(1) The ductility & damping reduction factor ( $C_{\mu h}$ ) has been proposed as an appropriate scaling factor which converts 5 %-damping elastic spectra into corresponding inelastic spectra for desired damping and ductility with a reasonable degree of approximation. Effects associated with damping and ductility are separately studied by introducing damping ( $C_h$ ) and ductility ( $C_\mu$ ) reduction factors.

(2) Site-dependent statistical models have been developed for estimating  $C_{\mu h}$ ,  $C_\mu$  and  $C_h$  on a hand calculator basis. Referent standard response ratio curves ( $\xi_r$ ) are modeled as high order polynomials enabling simple and efficient calculation of site-dependent inelastic response spectra for desired damping and ductility.

(3) Analyses performed for various soil conditions have demonstrated that  $C_{\mu h}$ ,  $C_\mu$  and  $C_h$  are site and period dependent (Figs.2, 7, 8 and 9). In particular, the strongest site and period dependence is found in the period region shorter than the overall predominant period range of ground motions considered. For longer periods, site and period dependence is less remarkable (Figs.9(b), 9(c) and 9(d)).

(4) Spectral behavior of  $C_\mu$  and  $C_h$  factors (Fig.8) is quite similar over the entire period range of 0.1s to 5s, therefore the amount of reduction associated with effects of ductility can be considered as an additional equivalent damping. However, it must be emphasized that with increasing ductility the overall effects of damping decrease.

(5) Parallel observations of results derived from the Montenegro and the Japanese strong motion data sets (Figs.9(a), 9(b), 9(c) and 9(d)) indicate that the subsoil conditions of sites where Montenegro records were taken are generally between the Japanese rock and diluvial sites.

## ACKNOWLEDGEMENTS

This study has been conducted during the stay of the first author in Japan, October 1982 ~ March 1984, under the International Course Program in the Field of Civil Engineering, Kyoto University. The support for his in stay in Japan as well as the travel support were provided by the Ministry of Education, Science and Culture (MONBUSHO), Japanese Government, which also supported this study in part under Grant in Aid for Scientific Research. These supports are gratefully acknowledged.

We extend our acknowledgements to the Institute of Earthquake Engineering and Engineering Seismology, IZIS-Skopje, University "Kiril and Metodij", Skopje, Yugoslavia for releasing the Montenegro Strong Motion Dataset. The Japanese strong motion data used herein have been published by the Port and Harbor Research Institute and the Public Works Research Institute, and baseline- and instrument corrected by using the method developed at Kyoto University<sup>1)</sup>.

Numerical computations have been performed on the FACOM M-382/M-380 Computer system of the Data Processing Center, Kyoto University.

## REFERENCES

- 1) Design Seismic Load Research Group (SGL) : Corrected and Integrated Earthquake Motion Accelerograms ; Graphical Information, Division of Structural Problems for Transportation Facilities, School of Civil Engineering, Kyoto University, March

- 1982.
- 2) Japan Road Association : Specifications for Highway Bridges, Part V Earthquake Resistant Design, 1980 (in Japanese).
- 3) Kameda, H. and Kohno, K. : Effect of Ground Motion Duration on Seismic Design Load for Civil Engineering Structures, Mem. Fac. Engg., Kyoto University, Vol.45 No.2, April 1983.
- 4) Kawashima, K., Aizawa, K. and Takahashi, K. : Estimation of Peak Ground Motions and Earthquake Response Spectra, (Part 5) Modification of Earthquake Response Spectra with Respect to Damping Ratio, Technical Memorandum of the Public Works Research Institute, No.2001, July 1983 (in Japanese).
- 5) Kawashima, K., Aizawa, K. and Takahashi, K. : Attenuation of Peak Ground Motion and Absolute Acceleration Response Spectra, to be presented at 8WCEE, July 21~28, 1984, San Francisco, California, U.S.A.
- 6) Milutinović, Z. and Kameda, H. : Equivalent Ground Acceleration (EQA) as an Engineering Seismic Hazard Parameter ; Development and Estimation, Research Report KUCE 83-ST-01, School of Civil Engineering, Kyoto University, Kyoto, December 1983.
- 7) Milutinović, Z. and Kameda, H. : Site-Dependent Response Amplification Spectra Scaled for Ductility and Damping ; Comparative Study of Japanese and Montenegro, Yugoslavia Strong Motion Data Sets, Research Report KUCE 84-ST-01, School of Civil Engineering, Kyoto University, Kyoto, April 1984.
- 8) Riddell, R. and Newmark, N. M. : Statistical Analysis of the Response of Nonlinear Systems Subjected to Earthquakes, Civil Engineering Studies, Structural Research Series No.468, University of Illinois, Urbana, August 1979.
- 9) Strong Motion Earthquake Accelerograms, Digitized and Plotted Data, Vol.I, II and III-Corrected Data, Report IZIIS-81-80, IZIIS-Skopje, Skopje, Yugoslavia.
- 10) Veletsos, A. S. and Newmark, N. M. : Effect of Inelastic Behavior on the Response of Simple Systems to Earthquake Motions, 2WCEE, Japan, 1960, Vol.II, pp.895 to 912.

(Received March 30 1984)

---